

Interaction Free Energy between Identical Spherical Colloidal Particles: The Linearized Poisson–Boltzmann Theory

STEVEN L. CARNIE AND DEREK Y. C. CHAN¹

Department of Mathematics, University of Melbourne, Parkville, Victoria, VIC 3052, Australia

Received March 12, 1992; accepted June 24, 1992

The linearized Poisson–Boltzmann theory is used to calculate the electrical double-layer interaction free energy between identical spherical colloidal particles. Results are given for interaction under conditions of constant surface potential, constant surface charge, and for the case in which charge regulation due to the dissociation of surface groups may be modeled by a linear relationship between the surface charge and the surface potential. Accurate results are obtained using a two-center expansion for the solution of the linearized Poisson–Boltzmann equation and numerical implementations of the algorithm are given for a full range of particles sizes, κa , and particle separations, κh . © 1993 Academic Press, Inc.

INTRODUCTION

Although the theory for the electrical double-layer interaction between colloidal particles has been established for more than half a century (1, 2), numerical evaluations of the free energies of interaction, even for spherical particles, are only available as approximate expressions such as the linear superposition approximation (3) (which is valid when the particles are far apart and the double-layer overlap is relatively weak). Alternatively, when $\kappa a \gg 1$ and $a \gg h$ (where a is the sphere radius, h the distance of closest approach between the spheres, and $1/\kappa$ is the Debye screening length of the electrolyte), one can use the Deryaguin construction to derive the interaction free energy between spheres from that between parallel plates (4). Part of the difficulty of calculating the interacting free energy is due to the nonlinear nature of the Poisson–Boltzmann theory which renders the problem analytically intractable except for the simplest geometries. However, in many practical problems, the surface potential of the particles is comparable to or only slightly larger than the thermal potential (kT/e) so that the linearized Poisson–Boltzmann theory still gives an acceptable qualitative and quantitative description of the system. As a consequence, it is desirable to have an accurate and convenient way to calculate the electrical double-layer interaction based on the linearized Poisson–Boltzmann theory.

While the theoretical framework for the analytic solution of the linearized Poisson–Boltzmann equation has been available for some time (1, 5), numerical calculation of the double-layer interaction free energy still requires specialized skills in analysis and numerical computations as well as adequate computational resources. With increasing computational power available on the current generation of desktop computers such calculations can now be placed within the capabilities of all colloid scientists provided an efficient implementation of the theory is available.

In this paper we provide an efficient method for calculating the double-layer interaction free energy between two identical spherical colloidal particles by solving the linearized Poisson–Boltzmann equation using a two-center expansion method. Here we consider (a) particles which maintain a uniform fixed surface potential during interaction—the constant potential model, (b) particles that maintain a uniform fixed surface charge density during interaction—the constant charge model, and (c) particles that, as a result of the chemical ionization of surface groups, maintain a known relation between the surface potential and surface charge—the regulation model. For this last model, the surface charge–potential relationship is in general nonlinear for a mass action type model for the dissociation of surface groups. This nonlinearity is inconsistent with the linearized Poisson–Boltzmann theory. However, we have shown elsewhere (6) that under appropriate conditions, it is possible to replace this charge–potential relation by a *linear* equation between the surface charge and the surface potential so that the method of solution for the cases of constant potential and constant charge models can be readily extended to the linearized regulation model to calculate the interaction free energy.

Previous work has used the two-center expansion method to calculate the interaction free energy between particles for the constant potential model (1) and also the force between particles for the constant potential, constant charge models (5), and for the linearized regulation model (7). It is always possible to obtain the interaction free energy at a given particle separation by (numerically) integrating the force curve but here we describe a direct method for calculating the interaction free energy that is more efficient.

¹ To whom correspondence should be addressed.

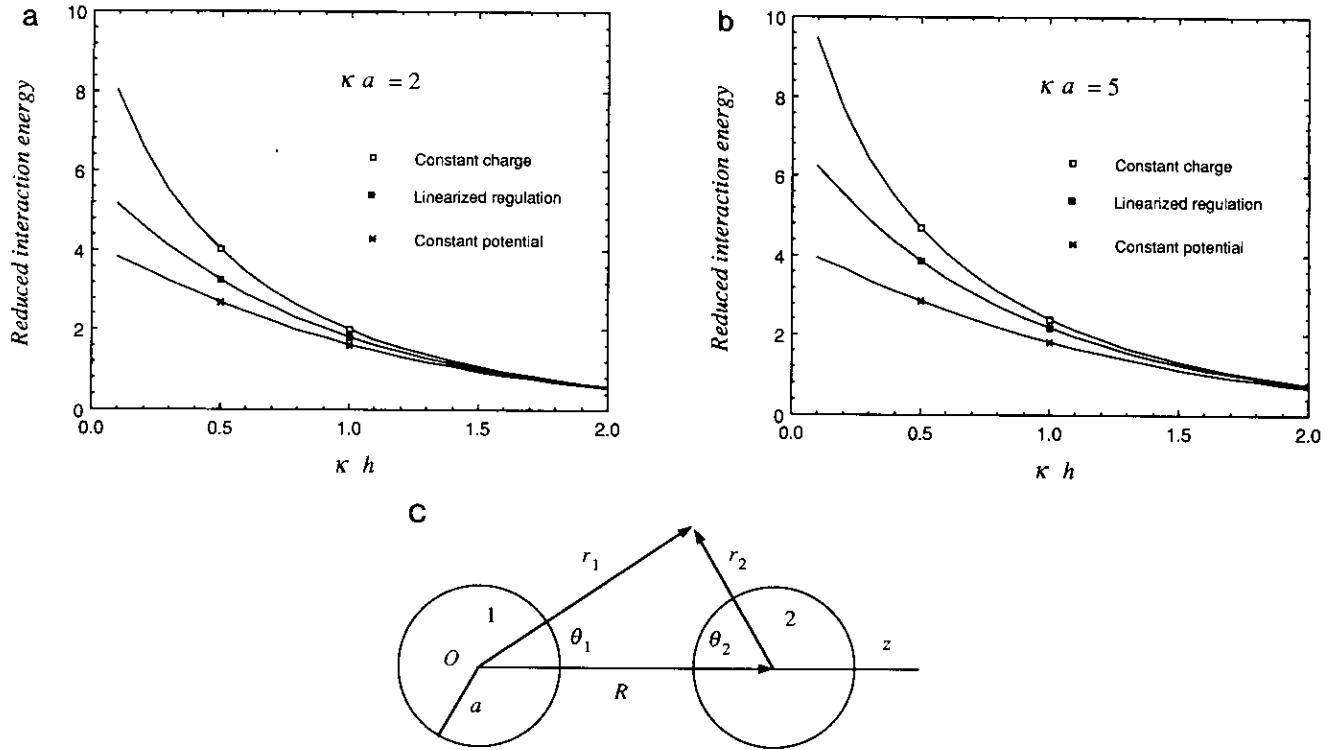


FIG. 1. Reduced interaction free energies, [45], as functions of separation for constant potential, constant charge, and linearized regulation [$(aK_2/\epsilon_0\epsilon_r) = 3$, $\epsilon_p = 0$] models at (a) $\kappa a = 2$ and (b) $\kappa a = 5$; (c) the coordinate system of two spheres.

Our calculation also accounts for the possibility of the particles having arbitrary dielectric constant ϵ_p which is relevant to cases (b) and (c) described above. Previous work (5, 7) only considered the special case $\epsilon_p = 0$. For the common case $\epsilon_p < 5$ in a highly polar solvent, the energy and force are well approximated by those for $\epsilon_p = 0$, but, since the analysis is only slightly complicated by allowing arbitrary ϵ_p , we retain the more general formulation here. Finally, we also present results for the variation of the surface charge and/or the surface potential on the particles as a function of position on the surface for a range of values of particle sizes and particle separations.

LINEAR POISSON-BOLTZMANN MODEL

In this section and the next, we follow the approach described in (5, 7) in order to make the paper self-contained.

In the linear Poisson-Boltzmann model the electrostatic potential ψ satisfies the equation

$$\begin{aligned} \nabla^2 \psi &= \kappa^2 \psi & r_1 > a \text{ and } r_2 > a \text{ (in the electrolyte)} \\ &= 0 & r_1 < a \text{ or } r_2 < a \text{ (inside the particles),} \end{aligned} \quad [1]$$

where κ is the inverse Debye length of the electrolyte and a is the radius of the particle (Fig. 1).

In the electrolyte, the solution of [1] can be written in the form (5)

$$\begin{aligned} \psi &= \sum_{n=0}^{\infty} a_n \{ k_n(\kappa r_1) P_n(\cos \theta_1) \\ &\quad + \sum_{m=0}^{\infty} (2m+1) B_{nm} i_m(\kappa r_1) P_m(\cos \theta_1) \}, \end{aligned} \quad [2]$$

where

$$B_{nm} = \sum_{\nu=0}^{\infty} A_{nm}^{\nu} k_{n+m-2\nu}(\kappa R) \quad [3]$$

$$A_{nm}^{\nu} = \frac{\Gamma(n-\nu+1/2)\Gamma(m-\nu+1/2)\Gamma(\nu+1/2)}{\pi\Gamma(m+n-\nu+3/2)(n-\nu)!(m-\nu)!} \times (n+m-\nu)!(n+m-2\nu+1/2) \quad [4]$$

R is the center-to-center separation between the two spheres, $\Gamma(z)$ is the gamma function, and $i_n(x)$, $k_n(x)$ are, respectively, the modified spherical Bessel functions of the first and third kind (8) and are related to the modified Bessel function of half integer order $I_{n+1/2}(x)$ and $K_{n+1/2}(x)$ by $i_n(x) = \sqrt{(\pi/2x)} I_{n+1/2}(x)$ and $k_n(x) = \sqrt{(\pi/2x)} K_{n+1/2}(x)$. To fa-

cilitate comparison with earlier work, we shall adopt as far as possible the notation in (5, 7) although we prefer to retain the present notation for the modified spherical Bessel functions. The solution given in [2] will decay to zero far from the spheres. Inside the spheres, the potential must be finite at $r = 0$ and so will have the general form

$$\psi = \sum_{n=0}^{\infty} b_n r^n P_n(\cos \theta), \quad [5]$$

where by symmetry $r = r_1$ or r_2 and $\theta = \theta_1$ or θ_2 . The unknown coefficients $\{a_n, b_n\}$ are found by applying the appropriate boundary conditions on the surface of the spheres. We now give in detail the equations that need to be solved to find the coefficients for constant potential, constant charge, and the linearized regulation model.

(a) *Constant Surface Potential Model*

When the potential on the surface of the spheres is uniform and remains fixed at ψ_{iso} (subscript iso denotes spheres in isolation) the solution inside the sphere [5] is not required and the coefficients a_n can be found by applying the condition $\psi = \psi_{\text{iso}}$ at $r_1 = a$. Using [2]–[4] this gives a system of linear equations

$$(\mathbf{L} + \mathbf{I})\mathbf{A} = \psi_{\text{iso}}\mathbf{e}, \quad [6]$$

where

$$\mathbf{A}_j = a_j k_j(\kappa a) \quad [7a]$$

$$\mathbf{L}_{jn} = (2j + 1)B_{nj} i_j(\kappa a) / k_n(\kappa a) \quad [7b]$$

$$\mathbf{e}_j = \begin{cases} 1, & j = 0 \\ 0, & j > 0 \end{cases} \quad [8a]$$

$$\mathbf{I}_{ij} = \begin{cases} 1, & j = i \\ 0, & j \neq i. \end{cases} \quad [8b]$$

These results are identical to those given in (5).

(b) *Constant Surface Charge Model*

When the spheres carry a uniform surface charge density σ that remains fixed at all particle separations, both the external solution [2] and the internal solution [5] for the potential ψ are required in general. The coefficients a_n and b_n are determined from the continuity of ψ (given by [2] and [5]) and the Gaussian boundary condition on the displacement field across the sphere surface at $r_1 = a$,

$$\left. \begin{array}{l} \psi \text{ continuous} \\ (\epsilon_p \nabla \psi^{\text{in}} - \epsilon \nabla \psi^{\text{out}}) \cdot \mathbf{n} = \sigma \end{array} \right\} \text{at } r_1 = a, \quad [9]$$

where $\epsilon = \epsilon_0 \epsilon_r$ is the product of the permittivity of free space,

ϵ_0 , and the relative permittivity of the solvent, ϵ_r , and ϵ_p is the corresponding product for the particle and \mathbf{n} is the unit outward normal at the surface of the sphere. The superscripts in (out) mean that the potential ψ is to be evaluated at $r_1 = a^-$ ($r_1 = a^+$).

The system of linear equations for the coefficient a_n now has the form

$$(\mathbf{L} + \mathbf{I})\mathbf{A} = (a\sigma/\epsilon)\mathbf{e}, \quad [10]$$

where

$$\mathbf{A}_j = \{j(\epsilon_p/\epsilon)k_j(\kappa a) - \kappa a k'_j(\kappa a)\} a_j, \quad [11a]$$

$$\mathbf{L}_{jn} = (2j + 1)B_{nj} \frac{j(\epsilon_p/\epsilon)i_j(\kappa a) - \kappa a i'_j(\kappa a)}{n(\epsilon_p/\epsilon)k_n(\kappa a) - \kappa a k'_n(\kappa a)}, \quad [11b]$$

and the coefficients b_j are given by

$$b_j = a^{-j} \{ a_j k_j(\kappa a) + \sum_{n=0}^{\infty} a_n (2j + 1) B_{nj} i_j(\kappa a) \}. \quad [12]$$

These equations reduce to those in (5) for the special case $\epsilon_p = 0$, which was the only case previously studied.

(c) *Linearized Regulation Model*

The most general form of a linear relation connecting the surface charge density and the surface potential that models surface ionization is given by

$$\sigma = K_1 - K_2 \psi, \quad [13]$$

where the sign of the constant K_1 is the same as the sign of the surface charge when the particle is in isolation. The constant K_2 is always positive: its magnitude reflects the ability of the surface ionization reactions to maintain a constant surface charge. For later reference, we call this constant the *regulation capacity* since it has the dimension of electrostatic capacitance per unit area (F/m^2). We defer further discussions of [13] regarding the choice of values for K_1 and K_2 to the Appendix: Linearized Regulation Model. We note that a similar boundary condition, referred to as the Robbins boundary condition, has been considered in a similar study of the forces between interacting spheres (7).

Applying the boundary conditions [9] together with [13], we find that the system of linear equations for the coefficient a_n is

$$(\mathbf{L} + \mathbf{I})\mathbf{A} = (aK_1/\epsilon)\mathbf{e}, \quad [14]$$

where

$$\mathbf{A}_j = \{ [j(\epsilon_p/\epsilon) + (aK_2/\epsilon)] k_j(\kappa a) - \kappa a k'_j(\kappa a) \} a_j \quad [15a]$$

$$\mathbf{L}_{jn} = (2j + 1)B_{nj} \times \frac{[j(\epsilon_p/\epsilon) + (aK_2/\epsilon)]i_j(\kappa a) - \kappa a i_j'(\kappa a)}{[n(\epsilon_p/\epsilon) + (aK_2/\epsilon)]k_n(\kappa a) - \kappa a k_n'(\kappa a)} \quad [15b]$$

while the coefficients b_j are still given by [12]. These equations reduce to those in (7) for the special case $\epsilon_p = 0$, which was the only case previously studied.

Provided $R > 2a$, the coefficients of the exterior solution a_n are found by truncating the matrix equations [6], [10], or [14] at an appropriate upper limit and solving the system of equations by direct numerical methods. The coefficients of the interior solution, b_n , for cases (b) and (c) are given by [12]. We defer discussion of the choice of the cutoff size of the system of linear equations until later in this paper. We now proceed to derive expressions for the force and interaction free energy in terms of the coefficients $\{a_n, b_n\}$ which appear in the spherical harmonic expansions of the potential outside [2] and inside the sphere [5].

FORCE

We can calculate the force acting on the particles by integrating the stress tensor

$$\mathbf{T} = (\Pi + \frac{1}{2}\epsilon E^2)\mathbf{I} - \epsilon \mathbf{E}\mathbf{E} \quad [16]$$

over a suitable surface. Here $\mathbf{E} = -\nabla\psi$ is the electric field and Π is the *difference* in the local osmotic pressure from that in the bulk electrolyte solution. In the linearized Poisson-Boltzmann theory this difference in osmotic pressure is related to the electrostatic potential by

$$\Pi = \frac{1}{2}\epsilon\kappa^2\psi^2. \quad [17]$$

If we want to evaluate the force on sphere 2 (due to the presence of sphere 1), we can choose any convenient surface S that encloses sphere 2 and perform the following surface integral to get the vector force on sphere 2

$$\mathbf{f} = \int_S \mathbf{T} \cdot \mathbf{n} dS, \quad [18]$$

where the unit normal \mathbf{n} at the surface S is directed toward sphere 2. Here we calculate the force on sphere 2 by choosing S to be the surface of sphere 1 ($r_1 = a$) so that \mathbf{n} will be the radius vector directed away from the center of sphere 1. By setting the origin of a Cartesian axis system at the center of sphere 1 and the z -axis to lie along the line joining the center of the spheres (Fig. 1), the *magnitude* of the force on sphere 2 in the z direction can be expressed as integrals over functions of the r and θ components of the electric field,

$$f = \mathbf{f} \cdot \mathbf{z} = 2\pi a^2 \epsilon \int_{-1}^1 \left\{ \frac{1}{2}[\kappa^2\psi^2 + E_\theta^2 - E_r^2]\mu + E_\theta E_r(1 - \mu^2)^{1/2} \right\} d\mu, \quad [19]$$

where the integrand is evaluated on the *outside* surface of sphere 1 ($r_1 = a^+$) and the integration variable μ is $\mu = \cos \theta_1$. Positive values of f imply a repulsion between the spheres.

(a) Constant Surface Potential Model

For the constant potential model, Eq. [19] for the repulsive force between the particles simplifies to

$$\begin{aligned} f &= -\pi a^2 \epsilon \int_{-1}^1 E_r^2 \mu d\mu \\ &= -\pi \epsilon (\kappa a)^2 \sum_{n=0}^{\infty} a_n \left\{ k_n' \sum_{p=0}^{\infty} a_p k_p' C_1(p, n) \right. \\ &\quad + 2k_n' \sum_{p=0}^{\infty} a_p \sum_{q=0}^{\infty} (2q+1) B_{pq} i_q' C_1(q, n) \\ &\quad + \left. \sum_{m=0}^{\infty} (2m+1) B_{nm} i_m' \sum_{p=0}^{\infty} a_p \right. \\ &\quad \left. \times \sum_{q=0}^{\infty} (2q+1) B_{pq} i_q' C_1(m, q) \right\}. \quad [20] \end{aligned}$$

The modified spherical Bessel functions in [20] are evaluated at $r_1 = a$ and

$$\begin{aligned} C_1(n, m) &= \int_{-1}^1 \mu P_n(\mu) P_m(\mu) d\mu \\ &= \begin{cases} \frac{2(m+1)}{(2m+3)(2m+1)}, & n = m+1 \\ \frac{2m}{(2m+1)(2m-1)}, & n = m-1 \\ 0, & n \neq m \pm 1. \end{cases} \quad [21] \end{aligned}$$

The expression for the force [20] differs from Eq. [9] of Glendinning and Russel (5) by a factor ($-\pi$) which was due to a typographical omission in (5). Also the expression given by Glendinning and Russel was for a nondimensional force,

$$F = f/(\epsilon\psi_{iso}^2), \quad [22]$$

so that to calculate F the coefficients a_n should be obtained by solving [6] with the surface potential ψ_{iso} set to 1 and then dividing the computed force f obtained from [20] by ϵ .

(b) Constant Surface Charge Model

For the constant charge model, the radial component of the electric field E_r is *not* constant on the outside surface of the sphere so the expression for the force [19] will not simplify as in the case $\epsilon_p = 0$ considered in (5). However, we can simplify the expression for the force by expressing it in terms of the electric field just *inside* the sphere using [9] together with the continuity of the tangential components of the field, E_θ , across the surface of the sphere

$$E_\theta^{\text{in}} = E_\theta(r_1 = a^-) = E_\theta(r_1 = a^+) = E_\theta^{\text{out}}. \quad [23]$$

The force [19] can be rewritten as

$$f = 2\pi a^2 \epsilon \int_{-1}^1 \left\{ \frac{1}{2} \left[\kappa^2 \psi^2 + E_\theta^2 - \left(\frac{\sigma}{\epsilon} + \frac{\epsilon_p}{\epsilon} E_r \right)^2 \right] \mu + E_\theta \left(\frac{\sigma}{\epsilon} + \frac{\epsilon_p}{\epsilon} E_r \right) (1 - \mu^2)^{1/2} \right\} d\mu \quad [24a]$$

$$= \pi \epsilon \int_{-1}^1 \left\{ \left[(\kappa a)^2 \psi^2 + (\partial\psi/\partial\mu)^2 (1 - \mu^2) - a^2 \left(\frac{\sigma}{\epsilon} - \frac{\epsilon_p}{\epsilon} \frac{\partial\psi}{\partial r} \right)^2 \right] \mu + 2a \frac{\partial\psi}{\partial\mu} \left(\frac{\sigma}{\epsilon} - \frac{\epsilon_p}{\epsilon} \frac{\partial\psi}{\partial r} \right) (1 - \mu^2) \right\} d\mu, \quad [24b]$$

where all quantities in the integrands are evaluated just *inside* sphere 1 ($r_1 = a^-$) and we have used the relations

$$E_\theta = \frac{1}{a} \frac{\partial\psi}{\partial\mu} (1 - \mu^2)^{1/2} \quad \text{and} \quad E_r = -\frac{\partial\psi}{\partial r} \quad [25]$$

with $\mu = \cos \theta_1$. The use of [24b] produces an expression for the force similar in form to that obtained for linearized regulation (see below). Explicitly, the force is

$$f = \pi \epsilon \left\{ \left(\frac{4b_1 a}{3} \right) \left(\frac{\sigma a}{\epsilon} \right) \left[\frac{\epsilon_p}{\epsilon} + 2 \right] + (\kappa a)^2 \sum_{n=0}^{\infty} b_n a^n \sum_{p=0}^{\infty} b_p a^p C_1(n, p) + \sum_{n=0}^{\infty} b_n a^n \sum_{p=0}^{\infty} b_p a^p C_3(n, p) - (\epsilon_p/\epsilon)^2 \sum_{n=0}^{\infty} n b_n a^n \sum_{p=0}^{\infty} p b_p a^p C_1(n, p) - 2(\epsilon_p/\epsilon) \sum_{n=0}^{\infty} n b_n a^n \sum_{p=0}^{\infty} b_p a^p C_2(n, p) \right\}, \quad [26]$$

where

$$C_2(n, m) = \int_{-1}^1 (1 - \mu^2) P_n(\mu) P'_m(\mu) d\mu = \begin{cases} \frac{-2m(m+1)}{(2m+3)(2m+1)}, & n = m+1 \\ \frac{2m(m+1)}{(2m+1)(2m-1)}, & n = m-1 \\ 0, & n \neq m \pm 1 \end{cases} \quad [27]$$

$$C_3(n, m) = \int_{-1}^1 \mu (1 - \mu^2) P'_n(\mu) P'_m(\mu) d\mu = \begin{cases} \frac{2m(m+1)(m+2)}{(2m+3)(2m+1)}, & n = m+1 \\ \frac{2m(m-1)(m+1)}{(2m+1)(2m-1)}, & n = m-1 \\ 0, & n \neq m \pm 1. \end{cases} \quad [28]$$

The integrals $C_2(n, m)$ and $C_3(n, m)$ are the same as in (5, 7). Although the expression for the force [26] now only involves a double rather than a triple sum as in earlier work (5), the coefficients $\{b_n\}$ must be evaluated via [12] and so the amount of work is the same in both cases.

(c) Linearized Regulation Model

The expression for the force in this case is very similar to the constant charge case (b). The only difference arises from the boundary condition [13]. So by replacing E_r^{out} by $\{\sigma/\epsilon + (\epsilon_p/\epsilon)E_r^{\text{in}}\}$ we get

$$E_r^{\text{out}} = \frac{K_1 - K_2 \psi^{\text{out}}}{\epsilon} + \frac{\epsilon_p}{\epsilon} E_r^{\text{in}}, \quad [29]$$

and this means that Eq. [26] can be used to calculate the force if we make the following replacements:

$$(\sigma a/\epsilon) \rightarrow (K_1 a/\epsilon) \quad \text{in the first term} \quad [30a]$$

$$\epsilon_p/\epsilon \rightarrow \epsilon_p/\epsilon + (aK_2/\epsilon) \quad \text{in the first term} \quad [30b]$$

$$(\epsilon_p/\epsilon) p b_p a^p \rightarrow b_p a^p [(p\epsilon_p/\epsilon) + (aK_2/\epsilon)] \quad \text{in the fourth term} \quad [30c]$$

$$(\epsilon_p/\epsilon) n b_n a^n \rightarrow b_n a^n [(n\epsilon_p/\epsilon) + (aK_2/\epsilon)] \quad \text{in the fourth and fifth term.} \quad [30d]$$

INTERACTION FREE ENERGY

While the expressions for the force between the particles are somewhat cumbersome, the expressions for the inter-

action free energy take on very simple forms. We calculate the interaction free energy for all three interaction models by a thermodynamic integration otherwise known as a coupling constant integration or charging procedure. This scheme has a very simple graphical representation in terms of the surface charge—surface potential relationships (11). For the linearized Poisson–Boltzmann model, the thermodynamic integrations are trivial. Furthermore, considerable algebraic simplification is afforded by judicious use of the $j = 0$ equation in the linear system for the unknown coefficient a_n [6, 10, or 14] to eliminate terms involving $\sum a_n B_{n0} = \sum a_n k_n(\kappa R)$. For later comparison between various models, we scale all energies by $(a\epsilon\psi_{\text{iso}}^2)$ where ψ_{iso} is the surface potential of a single sphere in isolation which is independent of the model for the surface charge or potential during interaction.

The interaction free energy between the two spheres with a distance of closest approach $h = R - 2a$ can be written as a sum of surface integrals over each sphere:

$$u(h) = 2(2\pi a^2) \int_{-1}^1 u(h, \mu) d\mu. \quad [31]$$

The first factor of 2 accounts for the fact that the surface integrals over sphere 1 and 2 are the same. The quantity $u(h, \mu)$ is the interaction free energy per unit area.

(a) Constant Surface Potential Model

The interaction free energy per unit area at constant surface potential, ψ_{iso} , is given by

$$u_p(h, \mu) = - \int_0^{\psi_{\text{iso}}} [\sigma_p(\psi, h, \mu) - \sigma_p(\psi, \infty, \mu)] d\psi \quad [32a]$$

$$= - \frac{1}{2} [G_p(h, \mu) - G_p(\infty, \mu)] \psi_{\text{iso}}^2. \quad [32b]$$

While [32a] is general for constant surface potential interactions, [32b] is only valid for the linearized Poisson–Boltzmann model with boundary condition $\psi = \psi_{\text{iso}}$ at $r_1 = a$ for which

$$\sigma_p(\psi, h, \mu) = G_p(h, \mu) \psi \quad [33]$$

with

$$G_p(h, \mu) = -(\epsilon\kappa/\psi_{\text{iso}}) \sum_{n=0}^{\infty} a_n \{ k'_n(\kappa a) P_n(\mu) + \sum_{m=0}^{\infty} (2m+1) B_{nm} i'_m(\kappa a) P_m(\mu) \}. \quad [34]$$

In the limit $h \rightarrow \infty$, B_{nm} (and hence L_{jn}) $\rightarrow 0$, and so $a_0 \rightarrow \psi_{\text{iso}}/k_0(\kappa a) = \kappa a \psi_{\text{iso}}/\sinh \kappa a$, while $a_n \rightarrow 0$ for $n > 0$.

After carrying out the integration in [31], we obtain

$$u_p(h) = 4\pi a \epsilon \psi_{\text{iso}}^2 \{ -(\pi/2)(a_0/\psi_{\text{iso}}) \text{csch } \kappa a + \kappa a + \kappa a \coth \kappa a \}. \quad [35]$$

The final answer depends on a_0 only through the ratio (a_0/ψ_{iso}) which can be obtained by solving [6] with $\psi_{\text{iso}} = 1$.

(b) Constant Surface Charge Model

The interaction free energy per unit area at constant surface charge, σ_{iso} , is given by

$$u_c(h, \mu) = \int_0^{\sigma_{\text{iso}}} [\psi_c(\sigma, h, \mu) - \psi_c(\sigma, \infty, \mu)] d\sigma \quad [36a]$$

$$= \frac{1}{2} [G_c(h, \mu) - G_c(\infty, \mu)] \sigma_{\text{iso}}^2, \quad [36b]$$

where [36b] follows from the linearized Poisson–Boltzmann model and boundary condition [9] where we have

$$\psi_c(\sigma, h, \mu) = G_c(h, \mu) \sigma \quad [37]$$

with

$$G_c(h, \mu) = \frac{1}{\sigma_{\text{iso}}} \sum_{n=0}^{\infty} a_n \{ k_n(\kappa a) P_n(\mu) + \sum_{m=0}^{\infty} (2m+1) B_{nm} i'_m(\kappa a) P_m(\mu) \}. \quad [38]$$

In the limit $h \rightarrow \infty$,

$$a_0 \rightarrow - \frac{(a\sigma_{\text{iso}}/\epsilon)}{\kappa a k'_0(\kappa a)} = (a\sigma_{\text{iso}}/\epsilon) \frac{2\kappa a \exp \kappa a}{\pi(\kappa a + 1)}, \quad [39]$$

while $a_n \rightarrow 0$ for $n > 0$.

Again, after the integration in [31] we get

$$u_c(h) = 4\pi a \epsilon \left(\frac{a\sigma_{\text{iso}}}{\epsilon} \right)^2 \left\{ \frac{\pi a_0}{2(a\sigma_{\text{iso}}/\epsilon)[\kappa a \cosh \kappa a - \sinh \kappa a]} - \frac{1}{1 + \kappa a} - \frac{1}{\kappa a \coth \kappa a - 1} \right\}. \quad [40]$$

As before, the interaction free energy depends on the coefficient a_0 only through the ratio $[a_0/(a\sigma_{\text{iso}}/\epsilon)]$, which can be obtained by solving [10] with $(a\sigma/\epsilon) = 1$.

(c) Linearized Regulation Model

The interaction free energy per unit area for spheres whose surface charge and surface potential are related by $\sigma = K_1 - K_2\psi$ is given by (11) (see also Appendix: Linearized Regulation Model).

$$u_r(h, \mu) = \left[-\int_0^{\psi_r(h, \mu)} \sigma_r(\psi, h, \mu) d\psi + \int_{\psi_r(h, \mu)}^{\psi^*} [K_1 - K_2\psi] d\psi \right]_{h=\infty}^h \quad [41a]$$

$$= [-\frac{1}{2}\sigma_r(h, \mu)\psi(h, \mu) + K_1\psi(h, \mu) - \frac{1}{2}K_2\psi^2(h, \mu)]_{h=\infty}^h \quad [41b]$$

$$= [-\frac{1}{2}[\epsilon_p\psi_r^{\text{in}}(h, \mu) - \epsilon\psi_r^{\text{out}}(h, \mu)]\psi^{\text{in}}(h, \mu) + K_1\psi^{\text{in}}(h, \mu) - \frac{1}{2}K_2[\psi^{\text{in}}(h, \mu)]^2]_{h=\infty}^h, \quad [41c]$$

where $\psi^* = K_1/K_2$ and [41b] follows from the boundary conditions [9], [13] which give the linear relation

$$\sigma_r(\psi, h, \mu) = G_r(h, \mu)\psi(h, \mu) \quad [42]$$

and allow us to do the integral over $d\psi$ in [41a]. In view of the continuity of the potential across the particle surface, we express the free energy per unit area in terms of the potential *inside* the sphere [5] in the form given by [41c] which will simplify the final expression for $u_r(h, \mu)$.

The integral over μ in [31] can be carried out to give the interaction free energy u_r for the linearized regulation model

$$u_r(h) = 4\pi\epsilon a \left\{ -(\epsilon_p/\epsilon) \sum_{n=0}^{\infty} \frac{n(b_n a^n)^2}{2n+1} + \kappa a \sum_{n=0}^{\infty} \frac{a_n k'_n(\kappa a)(b_n a^n)}{2n+1} + \kappa a \sum_{n=0}^{\infty} a_n \sum_{p=0}^{\infty} B_{np} i'_p(\kappa a)(b_p a^p) + 2b_0 \frac{aK_1}{\epsilon} - \frac{aK_2}{\epsilon} \sum_{n=0}^{\infty} \frac{(b_n a^n)^2}{2n+1} - \frac{(aK_1/\epsilon)^2}{[1 + \kappa a + (aK_2/\epsilon)]} \right\}, \quad [43]$$

where the last term comes from the contribution at $h = \infty$.

RESULTS

In order to compare results from the constant potential, constant charge, and linear regulation models, we follow Glendinning and Russel (5) and define a nondimensional force F by

$$F(h) = f(h)/(\epsilon\psi_{\text{iso}}^2) \quad [44]$$

and a nondimensional free energy of interaction U by

$$U(h) = u(h)/(a\epsilon\psi_{\text{iso}}^2), \quad [45]$$

where ψ_{iso} is the surface potential for an isolated sphere at h

$= \infty$. If the surface charge density of an isolated sphere σ_{iso} is prescribed, then ψ_{iso} is given by

$$\psi_{\text{iso}} = \frac{a}{1 + \kappa a} \frac{\sigma_{\text{iso}}}{\epsilon}. \quad [46]$$

For the linearized regulation model in which the parameters K_1 and K_2 are prescribed, the surface potential and charge of a sphere in isolation are given by

$$\psi_{\text{iso}} = \frac{K_1}{(\epsilon/a)(1 + \kappa a) + K_2} \quad [47]$$

$$\sigma_{\text{iso}} = \frac{(\epsilon/a)(1 + \kappa a)K_1}{(\epsilon/a)(1 + \kappa a) + K_2}. \quad [48]$$

For comparison with our calculations we list expressions for the force and interaction free energy derived using the linear superposition approximation and the Deryaguin approximation.

Linear Superposition Approximation—LSA

Force:

$$F_{\text{LSA}} = f_{\text{LSA}}/(\epsilon\psi_{\text{iso}}^2) = 4\pi(1 + \kappa R)(a/R)^2 \exp(-\kappa h). \quad [49]$$

Interaction free energy:

$$U_{\text{LSA}}(h) = u_{\text{LSA}}(h)/(a\epsilon\psi_{\text{iso}}^2) = 4\pi(a/R) \exp(-\kappa h). \quad [50]$$

Deryaguin Approximation—DA

Force:

$$F_{\text{DA}} = f_{\text{DA}}/(\epsilon\psi_{\text{iso}}^2) = \frac{2\pi\kappa a \exp(-\kappa h)}{1 + \eta \exp(-\kappa h)}. \quad [51]$$

Interaction free energy:

$$U_{\text{DA}}(h) = u_{\text{DA}}(h)/(a\epsilon\psi_{\text{iso}}^2) = \frac{2\pi}{\eta} \ln(1 + \eta \exp(-\kappa h)), \quad [52]$$

where

$$\eta = \begin{cases} 1 & \text{constant potential} \\ -1 & \text{constant charge} \\ \frac{aK_2/\epsilon - \kappa a}{aK_2/\epsilon + \kappa a} & \text{linearized regulation.} \end{cases} \quad [53]$$

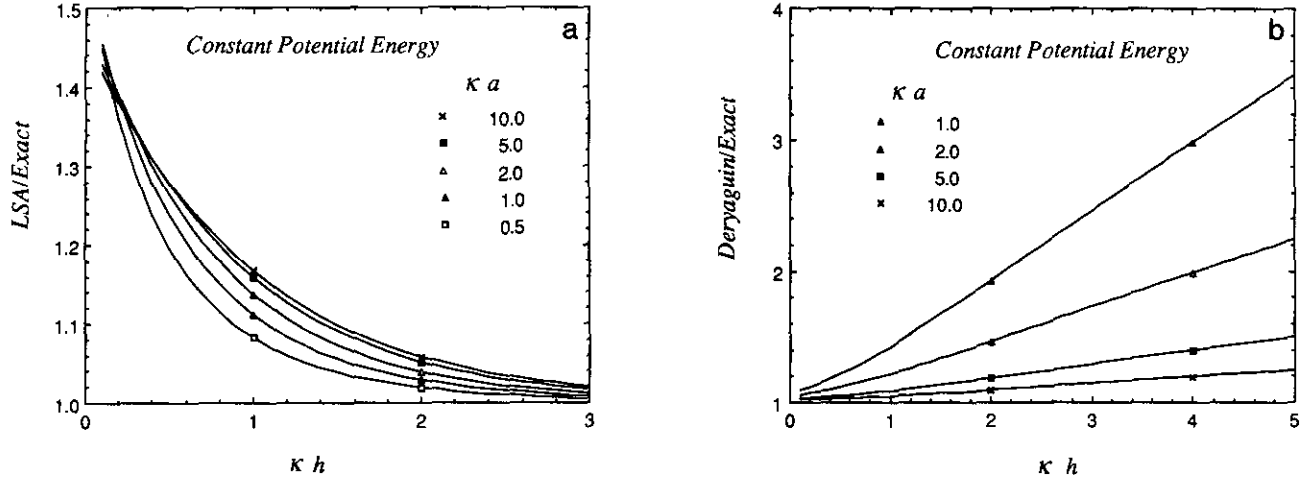


FIG. 2. The ratio of (a) the linear superposition and (b) the Deryaguin approximation to the exact interaction free energy under constant potential interaction.

For any given model, the force or the interaction free energy between the spheres can be computed by evaluating the infinite series given in the previous section. In practice, the number of terms, N_{\max} , we need to retain for the sum to give a prescribed level of accuracy depends on the value of κh and κa . Empirically we found that for four-figure accuracy for the energy or the force, we can use the formula

$$N_{\max} = \begin{cases} 5 & \text{if } h/a > 1 \\ \lceil 6\sqrt{a/h} \rceil & \text{if } h/a < 1, \end{cases} \quad [54]$$

where $\lceil x \rceil$ denotes the integer part of the real number x , to determine the value of N_{\max} . This choice of N_{\max} will of course control the size of the set of matrix equations we need to solve for the coefficients $\{a_n, b_n\}$ in the series expansion

for the potential. The matrix equations can be solved by direct methods (for example the LU factorization, which has complexity $O(N_{\max}^3)$). To calculate the energy from the coefficients $\{a_n, b_n\}$ the complexity is $O(1)$ for constant potential [35] or constant charge [40] interactions, and $O(N_{\max}^2)$ for the linearized regulation model [43]. To calculate the force, the complexity is $O(N_{\max}^2)$ for all cases. Thus the dominant part of the calculation lies in the solution of the system of linear equations for the coefficients $\{a_n, b_n\}$.

It is possible to symmetrize the matrix L , which in principle can lead to an improvement in the speed of the solution by a factor of 2 through the use of symmetric indefinite matrix solving algorithms (9). In practice, because we rarely need values of N_{\max} larger than 100, the computational overhead involved does not justify this refinement (10).

As checks on the validity of the analytic expressions for

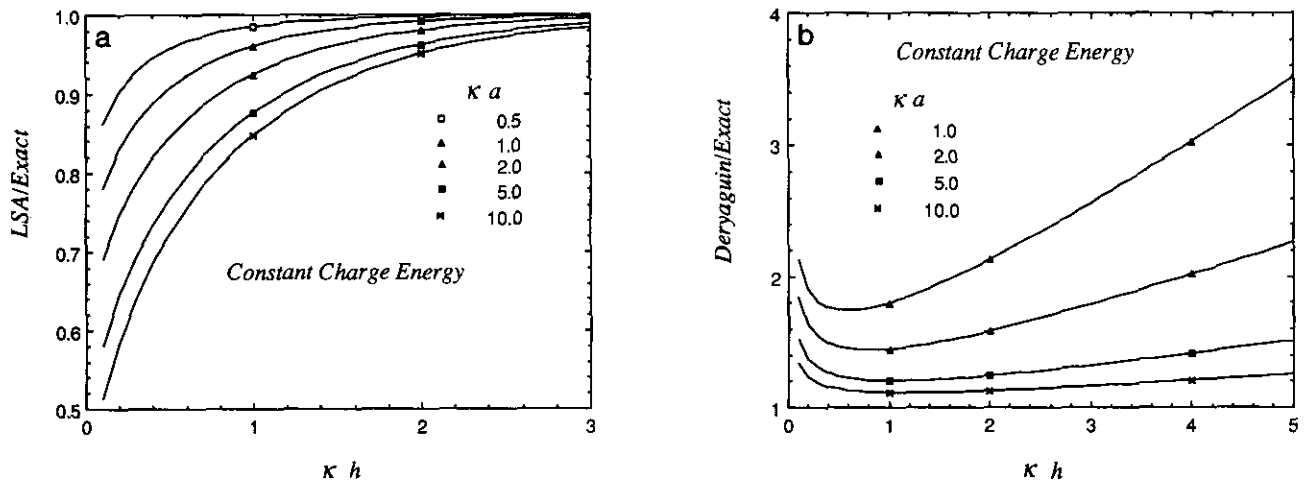


FIG. 3. The ratio of (a) the linear superposition and (b) the Deryaguin approximation to the exact interaction free energy under constant charge interaction with $\epsilon_p = 0$.

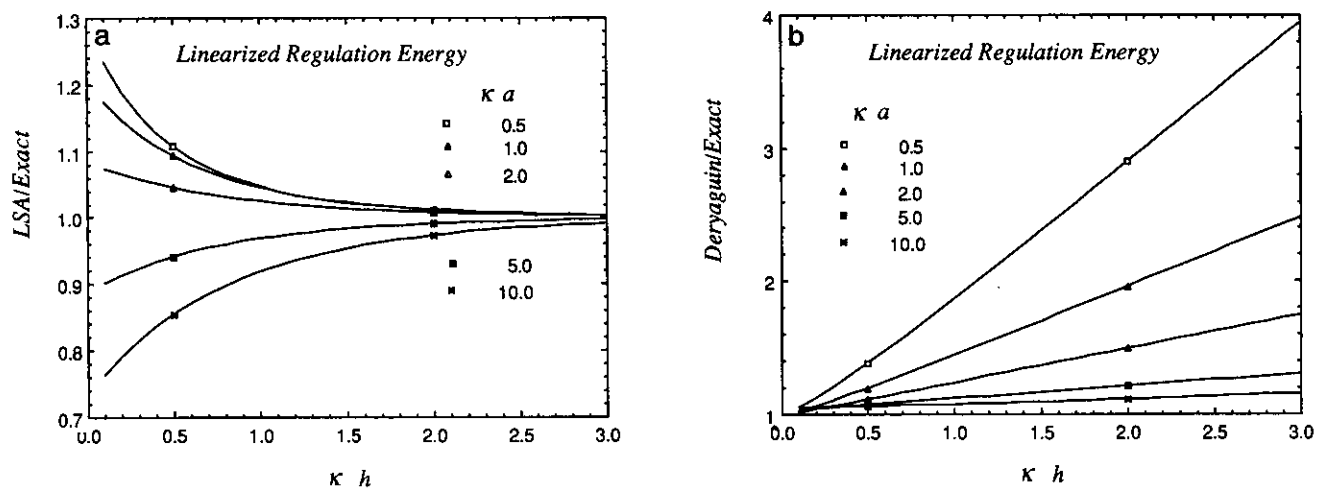


FIG. 4. The ratio of (a) the linear superposition and (b) the Deryaguin approximation to the exact interaction free energy under linearized regulation interaction with $(aK_2/\epsilon_0\epsilon_r) = 3$ and $\epsilon_p = 0$.

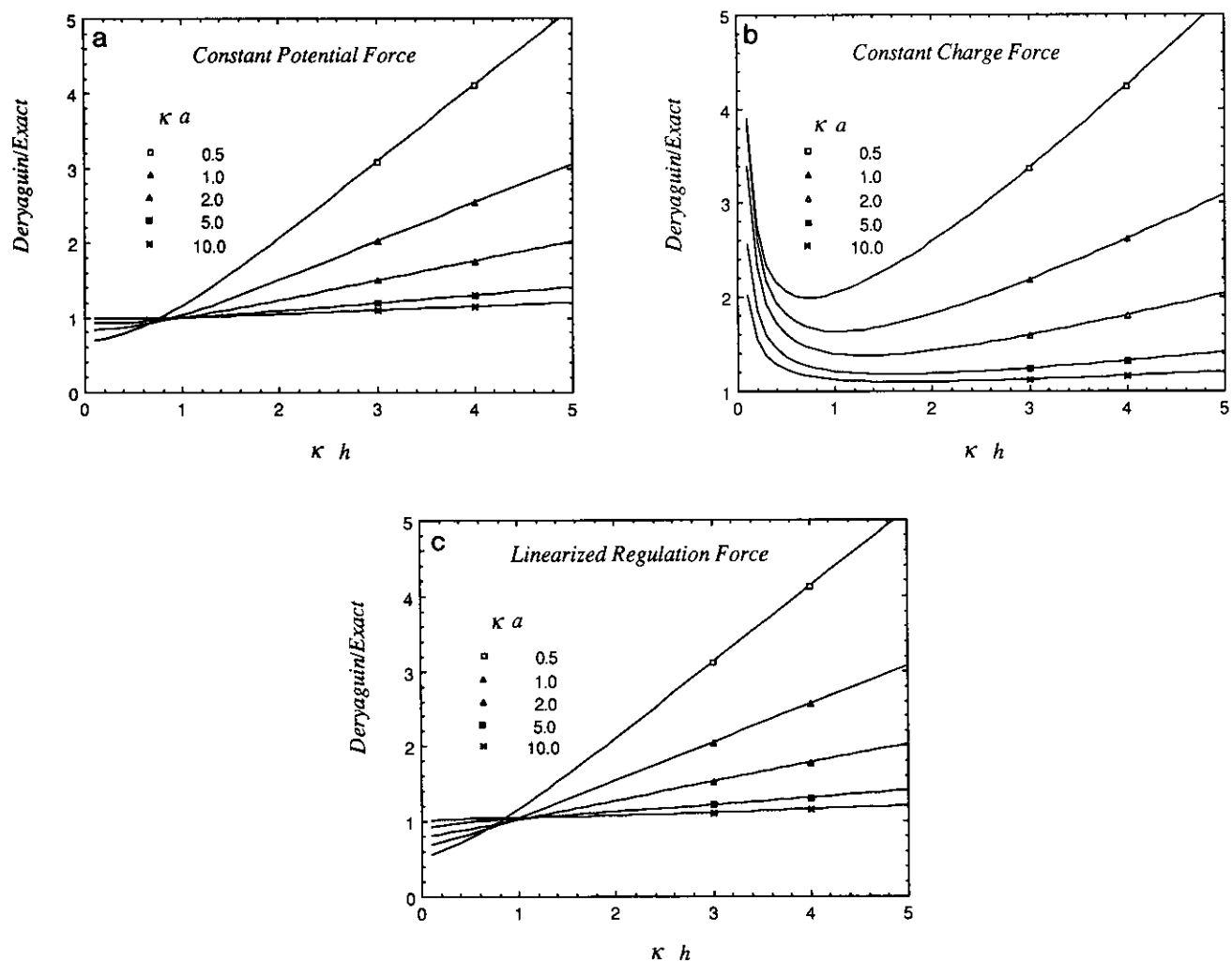


FIG. 5. The ratio of the Deryaguin approximation to the exact force under (a) constant potential, (b) constant charge, and (c) linearized regulation interaction with $(aK_2/\epsilon_0\epsilon_r) = 3$ and $\epsilon_p = 0$.

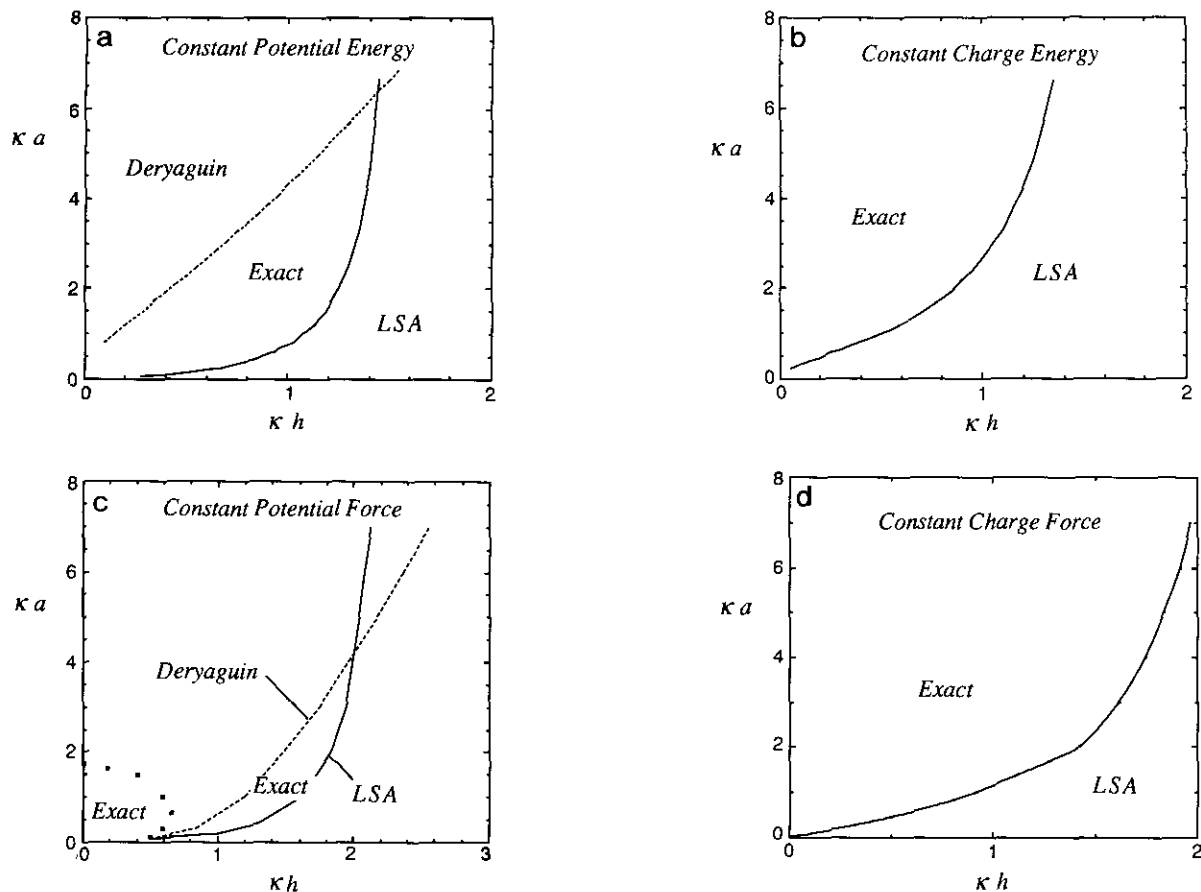


FIG. 6. Accuracy domains in $(\kappa a, \kappa h)$ parameter space for the linear superposition approximation and the Deryaguin approximation. The lines indicate where the approximate theories are within 10% of the exact result for (a) the interaction free energy at constant potential, (b) the interaction free energy at constant charge, (c) the force at constant potential, and (d) the force at constant charge [$\epsilon_p = 0$].

the force and the interaction free energy as well as on the numerical accuracy of our computations, we have performed numerical integrations of the calculated forces as functions of separation to verify that we do indeed recover the expected interaction free energies to within the known tolerance of the numerical integration algorithm.

In what follows, we present results for the cases of constant potential, constant charge, and linearized regulation. It is clear from [13] that the linearized regulation model interpolates between constant charge ($K_2 = 0$) and constant potential ($K_2 \rightarrow \infty$); changing the ratio (ϵ_p/ϵ) also has a similar effect, as is evident from [30]. Hereafter we choose a non-dimensional value for regulation capacity ($aK_2/\epsilon_0\epsilon_r$) = 3 which gives the intermediate behavior between constant potential and constant charge, at least for the range $\kappa a = 2$ to 5. This is demonstrated in Fig. 1 in which we compare the nondimensional or reduced interaction free energy [45] for the three models. Our use of the nondimensional parameter ($aK_2/\epsilon_0\epsilon_r$) to characterize the regulation capacity allows us to independently vary the regulation capacity, the electrolyte

concentration, and the particle separation. As expected, the interaction free energies for the three interaction models are significantly different from one another only for $\kappa h < 1$.

In Figs. 2–4 we examine the accuracy of the interaction free energy calculated according to the linear superposition approximation (LSA) and the Deryaguin approximation for the three interaction models: constant potential, Fig. 2; constant charge, Fig. 3; and linearized regulation, Fig. 4. On comparing Figs. 2a and 3a, we see that the LSA is an *overestimate* of the interaction free energy for constant *potential* interactions but an *underestimate* of the interaction free energy for constant *charge* interactions whereas for the linearized regulation model, with ($aK_2/\epsilon_0\epsilon_r$) = 3, the LSA can either overestimate or underestimate the interaction free energy depending on whether κa is small or large. Put another way, as κa increases the linearized regulation system goes from a constant potential behavior to a constant charge behavior. A similar trend can be observed in the comparison of the Deryaguin approximation for the three interaction models in Figs. 2b–4b. The increasing errors in the Deryaguin

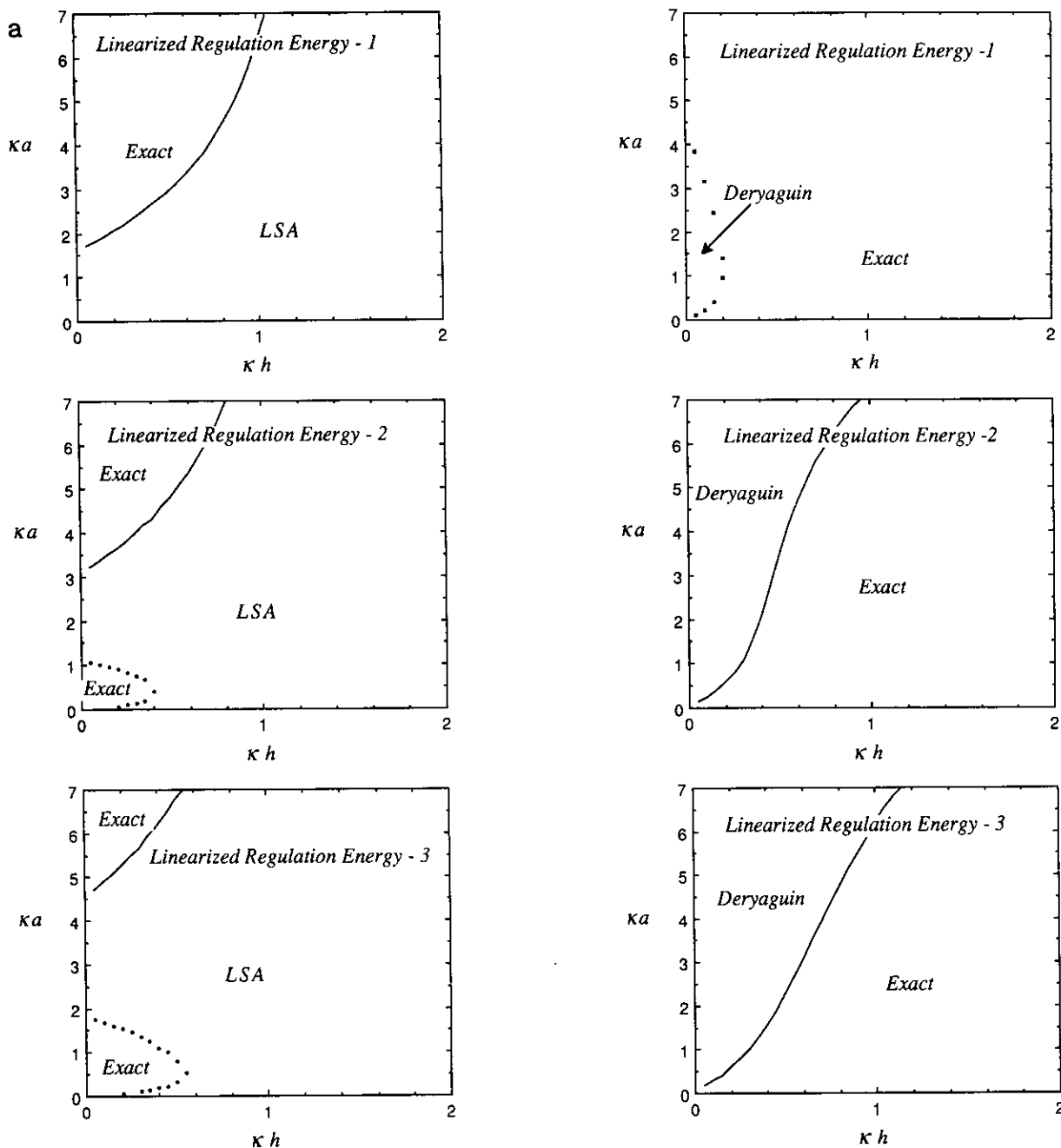


FIG. 7. Accuracy domains for the linearized regulation model in $(\kappa a, \kappa h)$ parameter space for the linear superposition approximation (left-hand column) and the Deryaguin approximation (right-hand column). The lines indicate where the approximate theories are within 10% of the exact result for (a) the interaction free energy and (b) the force. Values of $(aK_2/\epsilon_0\epsilon_r)$ are 1, 2, and 3 as indicated on the diagrams [$\epsilon_p = 0$].

approximation at small separations, $\kappa h < 0.3$, are due to its failure to properly account for the curvature effects on the spheres.

In Fig. 5 we examine the accuracy of the Deryaguin approximation at predicting the force between the spheres for the three interaction models with $(aK_2/\epsilon_0\epsilon_r) = 3$. Qualitatively, the behavior of the constant potential, Fig. 5a, and

linearized regulation, Fig. 5c, models are similar with both having a window in the region $\kappa h \sim 1$ where the Deryaguin approximation changes from an overestimate to an underestimate as κh decreases. On comparing Figs. 3b and 5b, pertinent to the constant charge model, we see that the Deryaguin approximation is less accurate in predicting the force than the interaction free energy. We note in passing that our

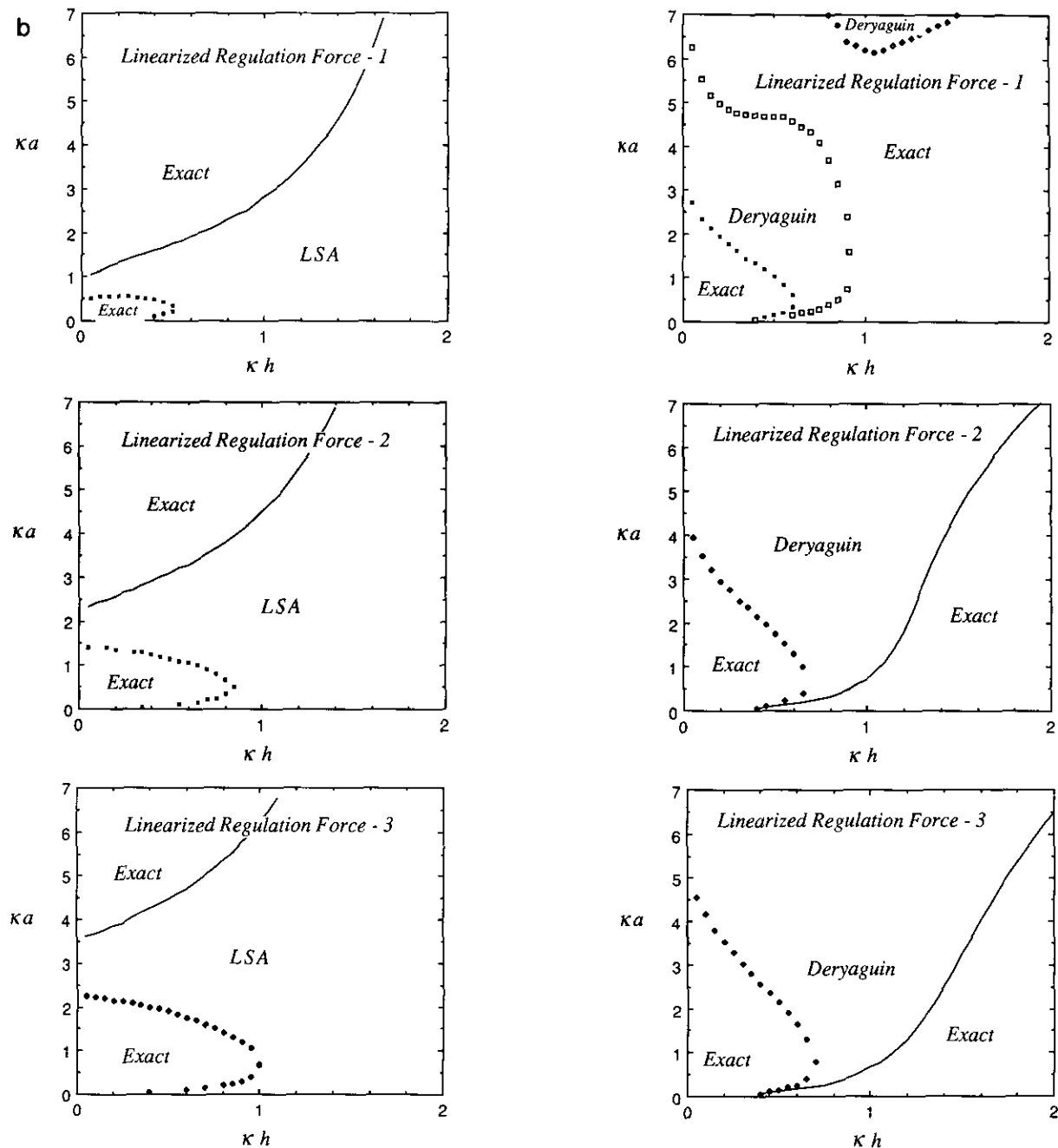


FIG. 7—Continued

result in Fig. 5b differs substantially from Fig. 6 of Glendinning and Russel (5)—we are able to establish correspondence between our results and all those in (5) except for this figure.

In order to assess the applicability of the Deryaguin approximation, the LSA and the full calculation given here, we delineate regions in $(\kappa a, \kappa h)$ parameter space where the results of the approximate methods are within 10% of the exact calculation—the same method of presentation as in (5, 7). The precise shape and location of these regions in $(\kappa a, \kappa h)$ parameter space varies with the model for the in-

teraction and also depends on whether one is considering the interaction free energy or the force. The results for the interaction free energy under constant potential and constant charge are shown in Figs. 6a and 6b. For calculating the interaction free energy under constant potential, Fig. 6a, the Deryaguin approximation is accurate even for quite modest values of κa provided κh is sufficiently small. On the other hand, for the constant charge model, Fig. 6b, the Deryaguin approximation is applicable only for large values of κa (> 10 , see also Fig. 3b). For calculating the force, Figs. 6c and 6d,

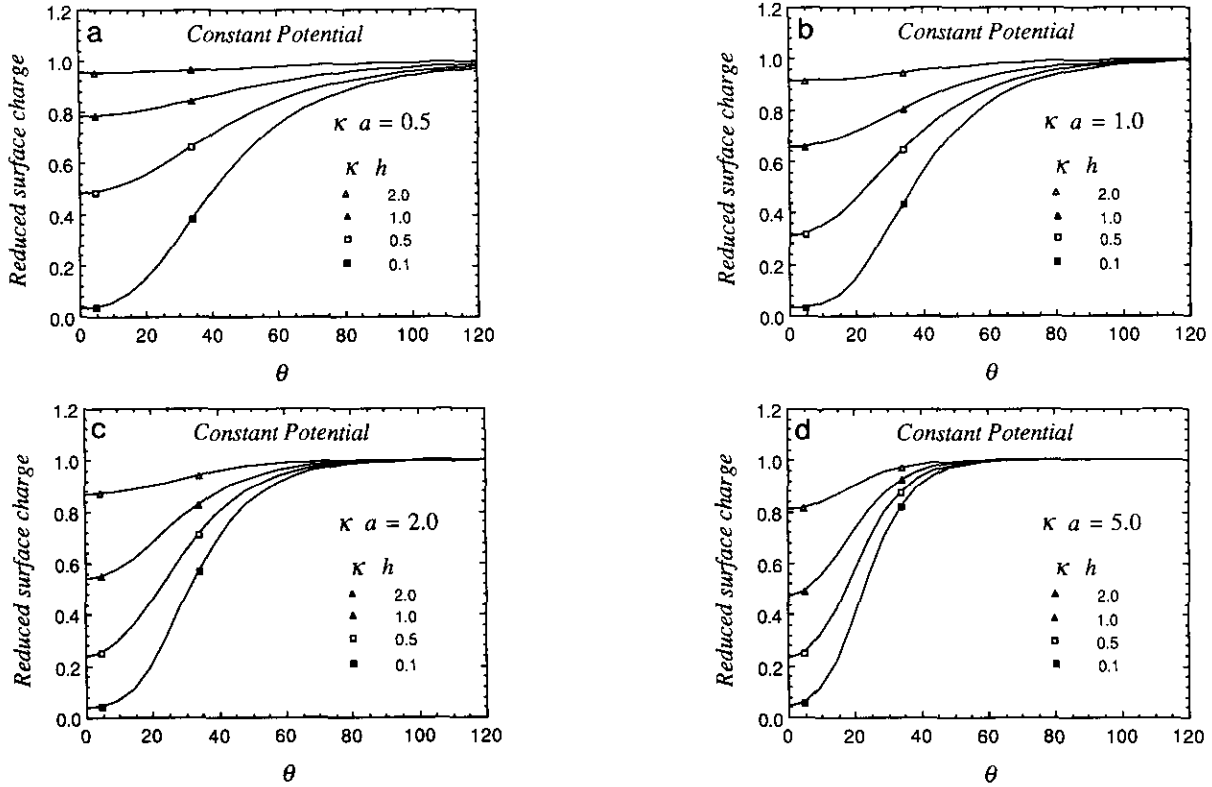


FIG. 8. Variation of the surface charge with the polar angle θ under constant potential interaction for (a) $\kappa a = 0.5$, (b) $\kappa a = 1.0$, (c) $\kappa a = 2.0$, and (d) $\kappa a = 5.0$. The surface charge is scaled by σ_{iso} .

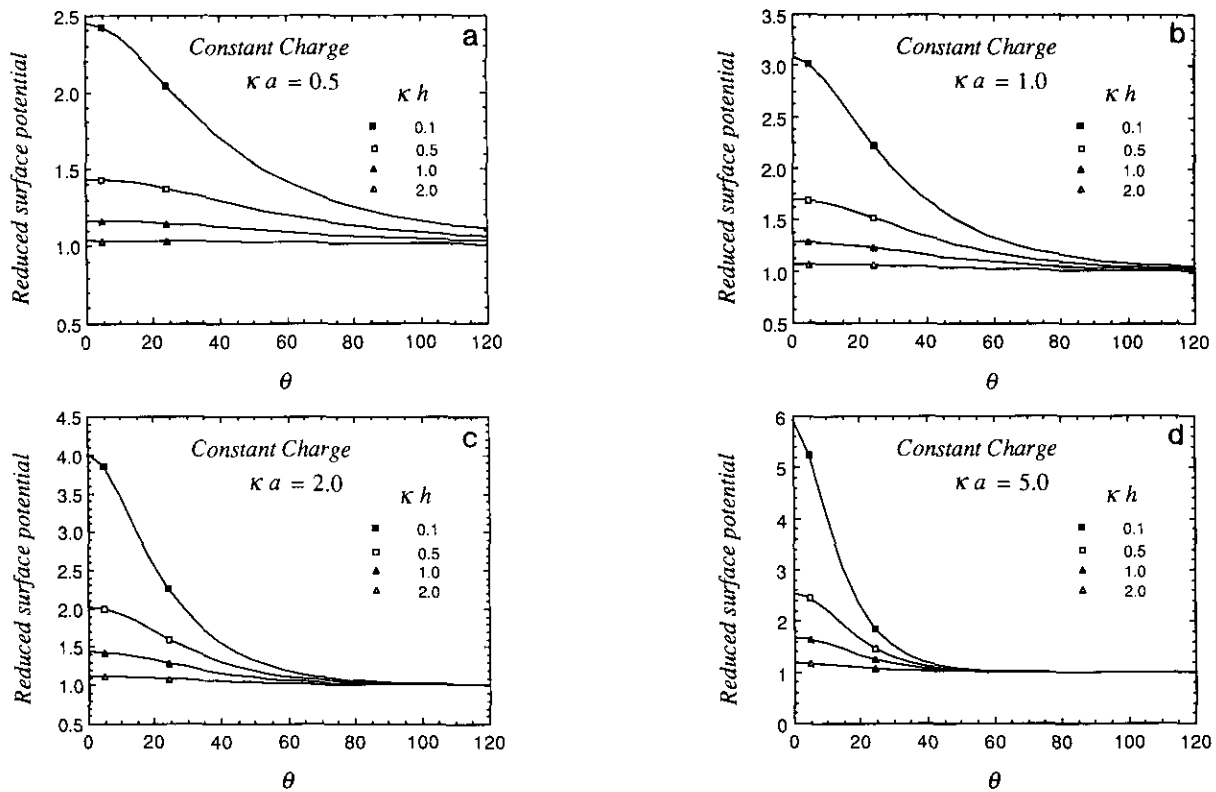


FIG. 9. Variation of the surface potential with the polar angle θ under constant charge interaction for (a) $\kappa a = 0.5$, (b) $\kappa a = 1.0$, (c) $\kappa a = 2.0$, and (d) $\kappa a = 5.0$. The surface potential is scaled by $\psi_{iso} [\epsilon_p = 0]$.

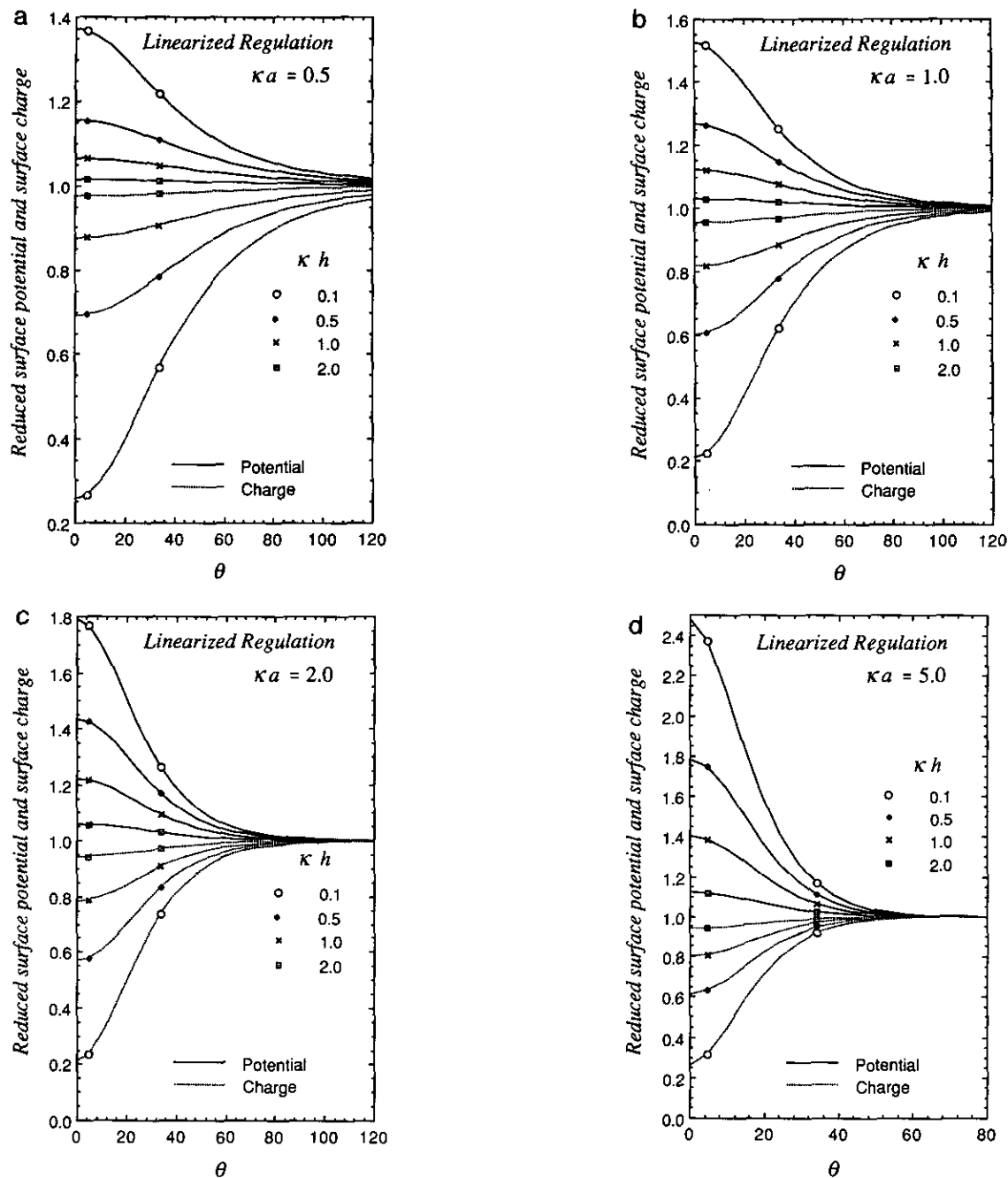


FIG. 10. Variation of the surface potential and surface charge with the polar angle θ under linearized regulation interaction [$(aK_2/\epsilon_0\epsilon_r) = 3$] for (a) $\kappa a = 0.5$, (b) $\kappa a = 1.0$, (c) $\kappa a = 2.0$, and (d) $\kappa a = 5.0$. The surface potential is scaled by ψ_{iso} , the surface charge is scaled by σ_{iso} [$\epsilon_p = 0$].

the regions of applicability of the LSA and of the Deryaguin approximation are similar in qualitative terms to that for the energy; however, there are quantitative differences in the size and location of the regions in κa and κh that require the use of the full theory. These differences for force and energy calculations are worth bearing in mind when it comes to choosing the appropriate approximate theory.

It is somewhat more complicated to delineate the accuracy domains for the linearized regulation model because we need

to consider the magnitude of the regulation capacity, K_2 . In what follows we present separately the accuracy domains of the LSA in the left-hand columns of Figs. 7a (energy) and 7b (force) and the accuracy domains of the Deryaguin approximation in the right-hand columns. The overall accuracy diagram, as in Figs. 6a and 6c, can be obtained by overlaying the two columns. Each column contains results for $(aK_2/\epsilon_0\epsilon_r) = 1, 2, \text{ and } 3$ which show intermediate behavior between constant charge ($K_2 = 0$) and constant potential ($K_2 \rightarrow \infty$).

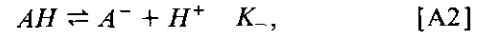
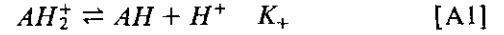
For values of K_2 in this range the LSA is unexpectedly accurate for all separations at intermediate values of κa ($2 < \kappa a < 5$) for both the energy and the force, see also Fig. 4a. In the case of the interaction energy, those regions of $(\kappa a, \kappa h)$ in which the LSA is inadequate can for the most part be accurately treated by the Deryaguin approximation. The same cannot be said for the force. In particular, in regions of low κa and κh we must use the exact calculation given here and elsewhere (7).

The series solution of the linearized Poisson–Boltzmann equation also allows us to obtain values for the potential and charge on the surface of the sphere. In Fig. 8 we show, for the constant potential model, the variation of the surface charge as a function of the angle θ —where $\theta = 0$ corresponds to the point of closest approach between the spheres, see Fig. 1. The reduced surface charge given in Fig. 8 is the surface charge divided by the surface charge when the spheres are infinitely far apart: $[\sigma(h, \theta)/\sigma_{\text{iso}}]$. We see that as the spheres approach, the surface charge is depressed and as κa increases to 5, only the charge on the portion of the spheres facing each other ($0 < \theta < 60^\circ$) is affected by the interaction. In Fig. 9, we show, for the constant charge model, the variation of the surface potential as a function of θ . The reduced potential is defined by: $[\psi(h, \theta)/\psi_{\text{iso}}]$. Here, we see that the potential rises above the potential on an isolated sphere. In this case, it is possible for the potential in the region between the spheres to become too large for the linearized Poisson–Boltzmann equation to hold. In the linearized regulation model, both the potential and the charge can change due to the double-layer interaction. These results are presented in composite diagrams in Fig. 10.

In summary, we have derived explicit formulas for the interaction free energy between identical spheres under the linearized Poisson–Boltzmann model for constant potential, constant charge, and the linearized regulation model. The results are readily implemented on desktop computers, the details of which can be obtained from the authors. We have made detailed comparisons between the present numerical results and the commonly used approximations: the Deryaguin and the linear superposition approximation for both the force and the interaction free energy. In the absence of a readily usable numerical method for solving the nonlinear Poisson–Boltzmann equation we hope that the results given here will serve as an indicator of the accuracy of the linear superposition approximation and the Deryaguin approximation when they are combined with the nonlinear Poisson–Boltzmann theory.

APPENDIX: LINEARIZED REGULATION MODEL

In this Appendix, we illustrate with a simple example how one may construct a linearized regulation model. Consider an amphoteric surface where the dissociation reactions,



with specified dissociation constants K_+ and K_- . If there are N_s such groups per unit area, the surface charge density can be written as (11)

$$\begin{aligned} \sigma_A(\psi) &= eN_s \frac{[AH_2^+] - [A^-]}{[AH] + [AH_2^+] + [A^-]} \\ &= eN_s \frac{\delta \sinh e(\psi_N - \psi)/kT}{1 + \delta \cosh e(\psi_N - \psi)/kT}, \end{aligned} \quad [A3]$$

where

$$\delta = 2(K_-/K_+)^{1/2} \quad [A4]$$

and

$$\psi_N = 2.303(kT/e) \left[\frac{1}{2}(pK_+ + pK_-) - pH \right] \quad [A5]$$

If the diffuse layer is treated in the linearized Poisson–Boltzmann approximation, the surface potential of such an amphoteric surface in isolation ψ_{iso} can be determined by solving the equation:

$$\begin{aligned} &(\epsilon\psi_{\text{iso}}/a)(1 + \kappa a) \\ &= eN_s \frac{\delta \sinh e(\psi_N - \psi_{\text{iso}})/kT}{1 + \delta \cosh e(\psi_N - \psi_{\text{iso}})/kT}. \end{aligned} \quad [A6]$$

We have shown elsewhere (6) that if we wish to approximate [A3] by a linear equation of the form [13], an accurate choice in so far as determining the interaction free energy is concerned is to replace [A3] by the tangent line located at ψ_{iso} , that is

$$\sigma_A(\psi) \approx \sigma_A(\psi_{\text{iso}}) + \left(\frac{\partial \sigma_A(\psi)}{\partial \psi} \right)_{\psi=\psi_{\text{iso}}} (\psi - \psi_{\text{iso}}). \quad [A7]$$

On comparison with [13] we can identify

$$K_1 = \sigma_A(\psi_{\text{iso}}) - \psi_{\text{iso}} \left(\frac{\partial \sigma_A(\psi)}{\partial \psi} \right)_{\psi=\psi_{\text{iso}}} \quad [A8]$$

and

$$K_2 = - \left(\frac{\partial \sigma_A(\psi)}{\partial \psi} \right)_{\psi=\psi_{\text{iso}}}. \quad [A9]$$

Now it is clear that K_2 has the dimensions of a capacitance per unit area. For other surface dissociation models, for example; surfaces with pure acidic, pure basic or zwitterionic

groups, the only change is the replacement of [A3] by the appropriate surface charge–surface potential relationship.

APPENDIX: NOMENCLATURE

a	sphere radius
a_n, b_n	coefficients in the two-center expansion of the potential, Eqs. [2] and [5]
K_1, K_2	parameters for the linearized regulation model, Eq. [13]
F	$= f(h)/(\epsilon\psi_{iso}^2)$, nondimensional force
f	force in newtons
h	distance of closest approach between the interacting spheres
U	$= u(h)/(a\epsilon\psi_{iso}^2)$, nondimensional interaction free energy
u	interaction free energy in joules
ϵ, ϵ_p	$\epsilon_0\epsilon_r, \epsilon_0\epsilon_{rp}$ = product of the permittivity of vacuum and the relative permittivity of the solvent (water), ϵ_r , or the particle, ϵ_{rp}
κ	Debye screening parameter
ψ_{iso}	surface potential of a sphere in isolation, volts
σ_{iso}	surface charge density of a sphere in isolation, coulombs per square meter.

ACKNOWLEDGMENT

This work is supported in part by the Advanced Mineral Processing Centre, a Special Research Centre funded by the Australian Federal Government at the University of Melbourne.

REFERENCES

1. Verwey, E. J. W., and Overbeek, J. Th. G., "Theory of the Stability of Lyophobic Colloids," Chap. 10. Elsevier, New York, 1948.
2. Deryaguin, B. V., and Landau, L. D., *Acta Phys. Chim. USSR* **14**, 633 (1941).
3. Bell, G. M., Levine, S., and McCartney, L. N., *J. Colloid Interface Sci.* **33**, 335 (1970).
4. Hogg, R., Healy, T. W., and Fuerstaneau, D. W., *Trans. Faraday Soc.* **62**, 1638 (1966).
5. Glendinning, A. B., and Russel, W. B., *J. Colloid Interface Sci.* **93**, 95 (1983).
6. Carnie, S. L., and Chan, D. Y. C., to be published.
7. Krozel, J. W., and Saville, D. A., *J. Colloid Interface Sci.* **150**, 365 (1992).
8. Abramowitz, M., and Stegun, I. A., "Handbook of Mathematical Functions." Dover, New York, 1965.
9. Golub, G. H., and Van Loan, C. F., "Matrix Computations," 2nd ed. Johns Hopkins Univ. Press, Baltimore, 1989.
10. Barwell, V., and George, A., *ACM Trans. Math. Software* **2**, 242 (1976).
11. Chan, D. Y. C., "Geochemical Processes at Mineral Surfaces," ACS Symposium Series No. 323, (J. A. Davis and K. F. Hayes, Eds.), p. 99, 1986.